

An essembled deep learning aproach for flow field prediction

Ali Dogan

Middle East Technical University
Cankaya, Ankara, Turkey
ali.dogan_04@metu.edu.tr

Adnan H. Dogan

Middle East Technical University
Cankaya, Ankara, Turkey
adnan.dogan@metu.edu.tr

ABSTRACT

In this paper, a machine-learning-driven method for predicting steady flow fields over the airfoil is presented based on Convolutional Neural Networks (CNN) and Multilayer Perceptron (MLP). The flow field around an airfoil plays a crucial step in aircraft design. In the classical approaches, the Navier-Stokes (NS) equations yield the flow field over an airfoil on a computational mesh with appropriate boundary conditions, known as computational fluid dynamics (CFD) techniques. However, they are computationally sluggish and expensive. Even though several machine-learning-driven models predict flow fields over an airfoil, they suffer from inconsistencies around the surface and high gradient regions. An essembled CNN-MLP model predicting a flow field of an airfoil is presented. CNN model with physical loss function focuses on solving the prediction errors of the high gradient areas, and MLP model is employed to obtain the flow field of the airfoil around its surface.

CCS CONCEPTS

• Machine Learning → Deep learning; • Fluid Mechanics → Aerodynamic.

KEYWORDS

datasets, neural networks, loss functions, assembly learning, aerodynamics

ACM Reference Format:

Ali Dogan and Adnan H. Dogan. 2022. An essembled deep learning aproach for flow field prediction. In *Proceedings of ACM Conference (Conference'17)*. ACM, New York, NY, USA, 6 pages. <https://doi.org/10.1145/nnnnnnn.nnnnnnn>

1 INTRODUCTION

With recent advancements, deep learning has opened many doors of opportunities for innovations in many areas. Fluid dynamics is one of those areas that deep learning methods offer alternative solutions to the computationally expensive fluid flow problems in a much faster way with accurate enough results compared to the widely used tools such as computational fluid dynamics (CFD). Flow field estimations are especially important in the time-consuming

optimization and design exploration studies such as airfoil selection phase of an aircraft design process.

An airfoil shape which gives the aircraft an ability to lift is selected accordingly by number of parameters such as flight regime, flight altitude, structural limits, maneuvering requirements and other constraints. Generally, the initial airfoil profile is selected from a particular family of airfoil sections based on the requirements. Some examples of these requirements are flight regime (i.e., supersonic, transonic, subsonic, and flight altitude), lift requirement, maneuvering and stall limits, drag limitations, and more. Initial design phases of the selection of an airfoil start with the calculation of the required wing area using the lift coefficient and drag-to-lift ratio of the selected airfoil so that the lifting surface fulfills the lift requirements in different flight conditions. However, modern aircraft wings are much more complex having various geometric characteristics such as taper ratio(s), sweep angle(s), aspect ratio, wing twist, dihedral angle, and more. Nevertheless, initial stages of aircraft design heavily relies on the airflows on 2D airfoils of the aircraft wing. In this phase, many experiments on different airfoil flow fields are tested.

Airflow fields are obtained using Computational Fluid Dynamics simulations. However, obtaining flow fields of a single airfoil is already a very time and energy consuming task. Hence, the amount of computing power is tremendous in these initial phases. Therefore, several studies are employed to develop a more robust and efficient approach to the design of aircraft lifting surfaces. In this study, we examine the deep learning approaches for the estimation of the flow fields around an airfoil and present an assembled deep learning model to overcome the two main problems encountered in many studies before: Information loss on the critical points of an airfoil during the transition from simulations to 2D grid; Lack of physical conservation laws on the deep learning models.

We aim to improve the results of flow fields on surface areas and high gradient regions by presenting an ensemble deep learning method to overcome the problem of poor results on the airfoil surfaces that is encountered in many studies [4, 9, 10]. We ensemble the CNNFOIL[4] model with additional physical law based loss functions and an MLP model trained on the surface areas to overcome the mentioned problems.

2 RELATED WORK

In recent years, several studies have focused on the prediction of the flow field around various object under diverse flow conditions with different methods including generative adversarial network (GAN), convolutional neural network (CNN), multi-layer perceptron (MLP) and graph neural network (GNN) models.

Guo et al. [5] achieved significant speedup with a CNN model for the prediction of velocity fields over 2D and 3D domains. [6] proposed a CNN model to predict velocity fields around a cylinder

Permission to make digital or hard copies of all or part of this work for personal or classroom use is granted without fee provided that copies are not made or distributed for profit or commercial advantage and that copies bear this notice and the full citation on the first page. Copyrights for components of this work owned by others than ACM must be honored. Abstracting with credit is permitted. To copy otherwise, or republish, to post on servers or to redistribute to lists, requires prior specific permission and/or a fee. Request permissions from permissions@acm.org.

Conference'17, July 2017, Washington, DC, USA

© 2022 Association for Computing Machinery.

ACM ISBN 978-x-xxxx-xxxx-x/YY/MM... \$15.00

<https://doi.org/10.1145/nnnnnnn.nnnnnnn>

for low Reynolds number flow. An encoder decoder CNN model was developed by Bhatnagar et al. [1] for the prediction of velocity and pressure fields around airfoils. Another CNN model based on U-net architecture was proposed by Chen et al. [2] for the flow field prediction around various arbitrary shapes in laminar flow. Zhang et al. [11] exhibited the success of CNN and MLP in variable flow conditions and object geometry of airfoils. They trained multiple CNN structures to learn the lift coefficients of the airfoils with various shapes in multiple Mach numbers, Reynolds numbers, and diverse angles of attack. In 2019, Lee et al. [7] applied four different deep learning networks; GAN and CNN with and without consideration of conservation laws. They analyzed the effects of the proposed physical loss functions and adversarial training on the predicted results. According to Lee, in estimating unsteady flow fields around airfoils on future occasions, deep learning models showed a good agreement with flow fields computed by numerical simulations. In the same year, Sekar et al. [10] concluded that the estimation of incompressible laminar steady flow fields over airfoils via the MLP model, the inputs of which are generated from a CNN parametrization architecture, is efficient and accurate. However, they stated that the estimations over the surface of the objects were poor due to lack of attention in those regions.

Peres et al. [3] introduced a hybrid approach to fluid flow problems by combining a (graph-based) neural network for robust estimations, with CFD-simulators for more accurate results in the physical sense. They have showed that the obtained combination performed better than the CFD simulation alone, and achieved a better generalization than a pure graph-network-based approach. In a recent study, Pfaff et al. [9] introduced a framework for learning mesh-based simulations with GNN architecture. They showed that GNN approach was able to outperform grid-based methods (CNNs) around the wingtips due to oversampling advantage with meshing. They concluded that flow field predictions over meshes demonstrates advantages even in flat 2D domains.

3 METHODOLOGY

3.1 Details on CNN Model

Numerical experiments are carried out to investigate the effect of loss functions on the flow field prediction around airfoils. Loss functions are implemented into the previously proposed model, CNNFOIL [4]. CNNFOIL, shown in Figure 1, is an encoder decoder CNN model that aims to predict pressure coefficient fields around airfoils for 0.7 Mach number flow at zero angle of attack. The Encoder part of the model, i.e. the convolution layers are employed to decompose the input and extract features, whereas the decoder part, i.e. the transposed convolution layers, are employed to construct a set of outputs from those features.

In the present study, CNNFOIL is trained with the solutions of Reynolds-averaged Navier-Stokes (RANS) based computational fluid dynamics (CFD) simulations for 204 different airfoil shapes in order to estimate density, x-component velocity and y-component of velocity around airfoils.

Three loss functions, namely L_2 , L_c and L_{gdl} , are used in the study. The contribution of each loss function to the base model is investigated by weighted combinations of L_c and L_{gdl} to the overall

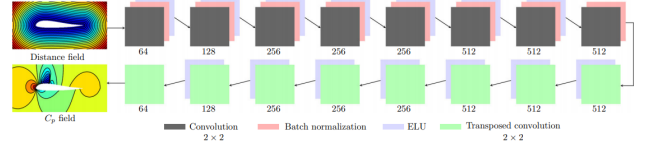


Figure 1: The illustration of the CNNFOIL architecture

loss function. The base model is trained with only L_2 loss function which can be expressed as follows:

$$L_2 = \sum_{n=1}^N [(\rho_n - \hat{\rho}_n)^2 + (u_n - \hat{u}_n)^2 + (v_n - \hat{v}_n)^2] \quad (1)$$

where ρ , u , v are the ground truth of density, x-component velocity and y-component of velocity, and $\hat{\rho}$, \hat{u} , \hat{v} is the model output of those flow variables. N is the number of data points in the flow field.

L_c loss function applied in the present study is derived from the continuity equation. L_c can be defined as follows

$$L_c = \sum_i \sum_j |(\rho_e u_e - \rho_w u_w) - (\hat{\rho}_e \hat{u}_e - \hat{\rho}_w \hat{u}_w)| + |(\rho_n u_n - \rho_s u_s) - (\hat{\rho}_n \hat{u}_n - \hat{\rho}_s \hat{u}_s)| \quad (2)$$

Notice that, each pixel of the solution image is treated as a conservation volume. For a cell centered approach, we need to interpolate for the face values for density and velocity. Flow variables on each cell face are estimated by averaging the corresponding values from the two opposite side of the cell face as

$$\begin{aligned} \Psi_e &= (\Psi(i, j) + \Psi(i + 1, j))/2 & \Psi_w &= (\Psi(i - 1, j) + \Psi(i, j))/2 \\ \Psi_n &= (\Psi(i, j) + \Psi(i, j + 1))/2 & \Psi_s &= (\Psi(i, j - 1) + \Psi(i, j))/2 \end{aligned} \quad (3)$$

where (i, j) denotes the cell indexes on the Cartesian grid.

Gradient Difference Loss, L_{gdl} is proposed by [8], penalizes the gradient differences and provides a smoother image in the predictions is defined by

$$L_{gdl}(Y, \hat{Y}) = \sum_{i,j} (|Y_{i,j} - Y_{i-1,j}| - |\hat{Y}_{i,j} - \hat{Y}_{i-1,j}|)^\alpha + (|Y_{i,j-1} - Y_{i,j}| - |\hat{Y}_{i,j-1} - \hat{Y}_{i,j}|)^\alpha \quad (4)$$

where $Y = \{\rho, u, v\}$ and $\hat{Y} = \{\hat{\rho}, \hat{u}, \hat{v}\}$ are the ground truth and prediction of flow variables, respectively. Parameter α is chosen to be 1 in all experiments.

In our experiments, the loss function is defined as the weighted combination of loss functions mentioned before. The obtained loss function is given as

$$Loss(Y, \hat{Y}) = \lambda_2 L_2 + \lambda_c L_c + \lambda_{gdl} L_{gdl} \quad (5)$$

The experimental matrix is listed in Table 1. In order to adapt the order of magnitudes of the loss functions, λ_c is chosen 100 in corresponding experiments.

3.2 Details on MLP Model

Previous studies in the literature [4, 10] indicate the fact that their proposed models may suffer from inconsistencies between the prediction and the ground truth of flow fields around the surface, simply because of the Cartesian nature of airfoils as their representation approximates with image pixels instead of meshes.

Table 1: Experiments

Experiment	λ_2	λ_c	λ_{gdl}
L_2	1	0	0
$L_2 + L_c$	1	100	0
$L_2 + L_{gdl}$	1	0	1
$L_2 + L_c + L_{gdl}$	1	100	1

The Multi-Layered Perceptron (MLP) model is implemented to remedy the deficiency of the model's prediction over the surface of airfoils. The model takes the airfoil embedding¹ as input and produces the flow fields around the airfoil's surface.

However, The model itself alone does not solve the problem but brings another issue to light. That is, the prediction airfoil embedding from an input source. Therefore, for generating the parameters for the airfoils' shape, numerous methods are utilized in search of a better result.

3.2.1 CNN-Based Parametrization. The CNN Autoencoder Model with three hidden layers and 16 parameters predicts 70 y-locations of the airfoil's surface in the XY-plane, whose x-locations are pre-defined and unchanged for all. It is designed so that those 16 parameters inputs the MLP model for predicting flow fields of that airfoil over the surface.

3.2.2 MLP-Based Parametrization. The Bezier curve is a parametric curve, where it could be uniquely composed into its ordered Bezier points. The number of Bezier points determines the class of its producing Bezier curve, such as linear, quadratic, or cubic curves, and so on. Numerous Bezier points could draw a more sinusous Bezier curve, whereas this grow-up causes the computational cost to increase exponentially. At this point, The Bezier Curve Estimation Network is utilized as an alternative approach to the conventional Bezier curve and point computation methods in a much faster and simpler way with accurate-enough results.

4 DATA PREPARATION

Data preparation is crucial for both standardizing model's input and output dataset, as well as it might well enhance the model's training and testing performance better. For airfoil representations, NACA² hosts a dataset of over one and half thousand airfoil shape, each of which consists of different number of xy-coordinates at which the airfoil's surface intersects. However, both MLP and CNN-Autoencoder models expect its input data to be of fixed amount. Different experiment setups are prepared for those different models.

4.0.1 CNN-Autoencoder Parametrization. More sophisticatedly, The encoder part of the model takes a grey-scaled 216x216x1 image frame of an airfoil, as in figure 2, and decomposes it into 16 parameters, whereas the decoder reconstructs the shape of the airfoils from those parameters in-between. Here, the MLP model is intended to take those parameters and generate the flow fields of that airfoil over the surface itself. For the input image, the distance of a pixel to the nearest point on the airfoil is scaled between 0 and 255, where

¹of an airfoils' parameters to draw itself

²National Advisory Committee for Aeronautics

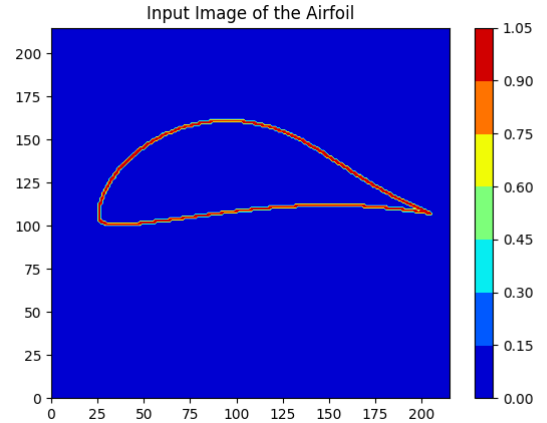


Figure 2: A image of the airfoil E435 for the Autoencoder Model

255 indicates a distance of $\sqrt{2}$ pixel or more. Therefore, only the pixels in the vicinity of the airfoil's surface have a value lower than 255.

4.0.2 MLP-Bezier Estimation. MLP model takes seventy upper and seventy lower y-locations of the airfoil's surface whose x-locations are constant through all samples in the dataset, as in figure 3, and produces six upper and six lower Bezier points that can construct the airfoils' shape back. For understanding the Bezier curve estimation mechanics via DL-based methods, numerous models with different hyperparameters, such as number of layers, number of nodes, and activation methods, are tested, resulted in figure 10. It is concluded that converting the bezier points, outputted from the Bezier Curve Estimation Model, back to a curve with which loss function compares the airfoil's shape, as ground truth, increases overall performance.

4.0.3 Flow-Field Prediction.

5 RESULTS AND DISCUSSION

Our results consist of three main parts. First, experiments on the CNN model are employed with different loss functions to investigate their effects on the flow field prediction. Second, MLP model is employed and discussed. Finally, the integrated model for the prediction of flow fields is examined and discussed.

5.1 CNN Model

Training history of each case in Table 1 with respect to each error function given in Eq. 1, Eq. 2 and Eq. 4 are depicted in Figure 4, Figure 5 and Figure 6, respectively. Figure 4 shows that combining L_2 loss function with L_c or L_{gdl} loss functions does not provide a strong contribution to minimizing the L_2 error function. However, implementing L_c or L_{gdl} loss functions into L_2 loss function have significant effect on the convergence of mass conservation as can be seen in Figure 2. Even, just adding the L_{gdl} loss function may help to satisfy mass conservation than L_2 loss function by itself.

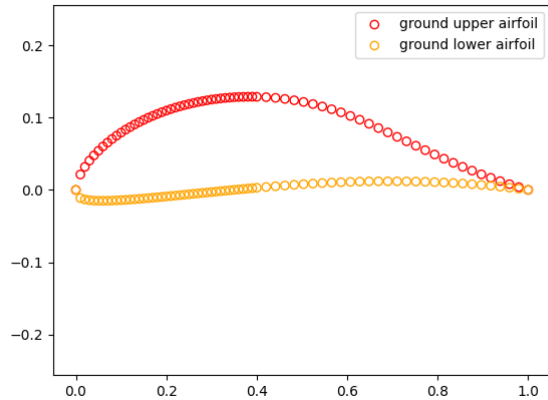


Figure 3: A set of points scattered through the airfoil's surface E435 for the Bezier Point Estimation Network

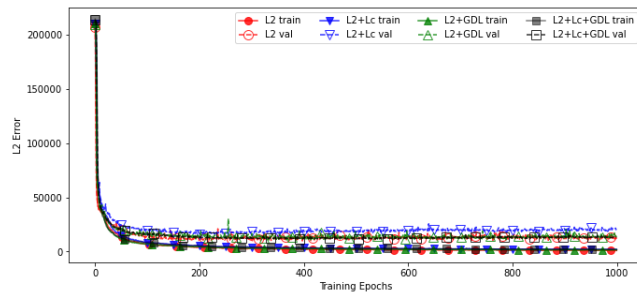


Figure 4: Convergence history of L_2 error function

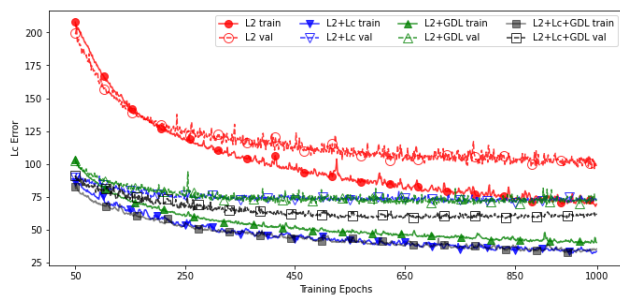


Figure 5: Convergence history of L_c error function

Figure 4 shows the convergence history of L_{gdl} during the training of each case in Table 1. Figure 4 demonstrates better convergence history of L_{gdl} for the cases in which the L_{gdl} loss function appeared. However, adding L_c loss function has an adverse effect on the L_{gdl} errors by resulting in much more L_{gdl} error than L_2 loss function by itself.

Furthermore, density, x -component velocity and y -component of velocity fields of an airfoil from the test set are compared for each case in Table 1 in Figure 7, 8 and 9, respectively. The ground

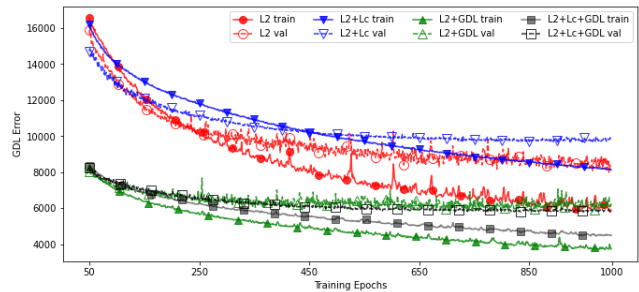


Figure 6: Convergence history of L_{gdl} error function

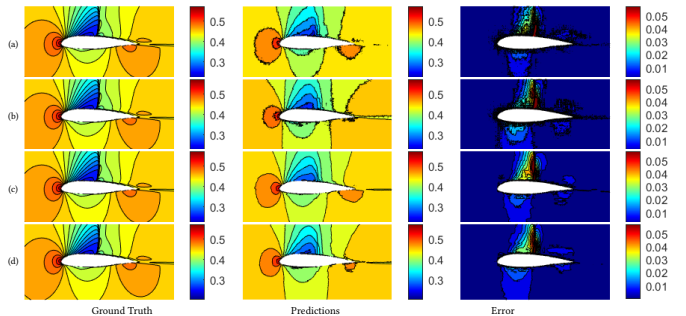


Figure 7: Density fields of LS 417 airfoil from the test set. Left column: ground truth extracted from CFD simulations, Middle column: the model output, Right Column: the absolute difference of density fields between the model output and the ground truth for (a) L_2 , (b) $L_2 + L_c$, (c) $L_2 + L_{gdl}$, (d) $L_2 + L_c + L_{gdl}$.

truth, the prediction and the absolute error between the ground truth and the prediction for the density, x -component velocity and y -component of velocity fields are plotted in Figure 7, 8 and 9. Even though combining L_c and/or L_{gdl} loss functions with L_2 loss function improves L_c and L_{gdl} errors as shown in Figure 5 and 6, the loss combination cases do not perform better than the case in which only L_2 loss function is included. This may also demonstrate that L_2 error function is enough to meet the convergence criteria for the training of a deep learning model. However, we can observe smooth contour lines in the cases in which L_{gdl} loss function appeared and the adverse effect of L_c loss function on the L_{gdl} errors mentioned before. Apart from the loss function comparison, the model performs reasonably well in flow field prediction for three flow variables except the shock waves as can be seen in the absolute errors in Figure 7, 8 and 9.

5.2 MLP Model

Predicting the flow fields over the airfoil's surface via a completely different model, rather than as a part of the model, increases the model's overall performance as a whole compared to the previous attempts in the literature. For that purpose, the MLP model is appointed and equipped with either of two different parametrization methods for extracting the embeddings of an airfoil's shape, called Bezier Point Estimation and CNN Autoencoder.

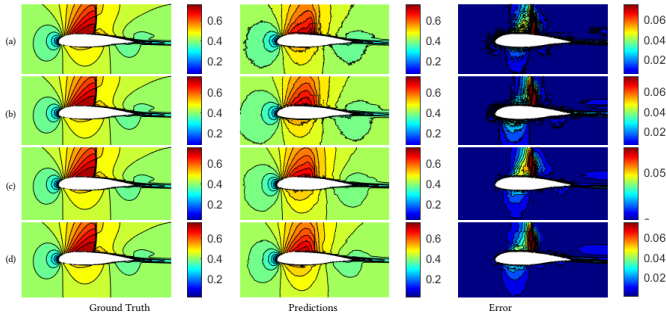


Figure 8: x -component velocity fields of LS 417 airfoil from the test set. Left column: ground truth extracted from CFD simulations, Middle column: the model output, Right Column: the absolute difference of density fields between the model output and the ground truth for (a) L_2 , (b) $L_2 + L_c$, (c) $L_2 + L_{gdl}$, (d) $L_2 + L_c + L_{gdl}$.

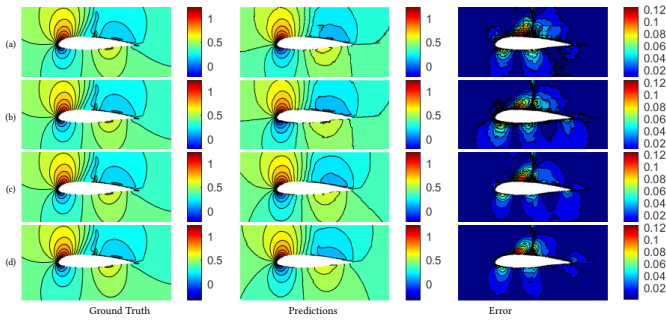


Figure 9: y -component velocity fields of LS 417 airfoil from the test set. Left column: ground truth extracted from CFD simulations, Middle column: the model output, Right Column: the absolute difference of density fields between the model output and the ground truth for (a) L_2 , (b) $L_2 + L_c$, (c) $L_2 + L_{gdl}$, (d) $L_2 + L_c + L_{gdl}$.

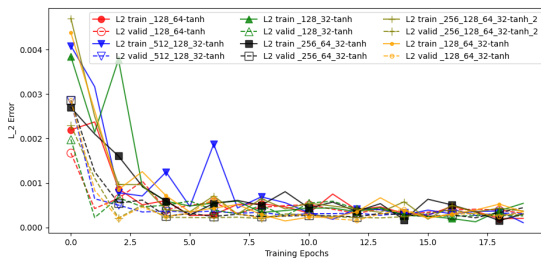


Figure 10: MSE Convergence of Bezier Point Prediction MLP Models with different hyperparameters

Numerous experiments are conducted to observe the effects of those methods on the MLP model. Figure 10 integrates loss functions for several hyper-parameter configurations. Training history of each approach is given in the figure 10 and 11.

With the Autoencoder model, the MLP model is fed by the 16 parameters at the end of the encoder part of the Autoencoder, and its output is compared with the skin friction data (C_f) of the airfoil

over the surface. An example input-output pair is given in figure ??, where red dots are XY-coordinates of ground truth, and the colored lines are the upper and lower surfaces of the airfoil predicted by the Autoencoder Model. Finally, figure 11 shows the model converges within a thousand epochs with 1550 airfoil samples.

In Bezier Point Estimation MLP Model, on the other hand, skin friction of the airfoil data is used to obtain 6 upper and 6 lower bezier point. However, the Bezier Point Estimation Model has not optimized yet due to the variety of mathematical and geometric properties of bezier points. Therefore, deriving airfoil shapes from the obtained bezier points result in poor airfoil shapes in some airfoils.

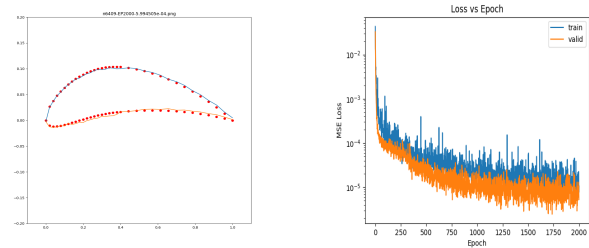


Figure 11: MSE Convergence History of Autoencoder Model

As seen, the Autoencoder model produces more useful parameters than the MLP model's prediction, which correlates with their training performances

6 CONCLUSION

In the present study, we looked at the two main problems that are encountered in the flow field prediction tasks. We investigated the role of loss functions utilized in deep neural network models for fluid flow studies by implementing them on previously proposed CNNFOIL model. Initial findings show additional loss functions did not improve the flow field predictions significantly in terms of L2 error. However, the loss combinations helped to satisfy conservation of mass and edge smoothing in the flow fields. A comprehensive investigation will continue by also examining the conservation of momentum and energy. Furthermore, conducting experiments on other neural network models may help to see more distinct results. Under the MLP model, we focused on the representation of an airfoil and its feature extraction. Later, we conducted two models to obtain a better representation of airfoils so that further deep learning models can be employed to focus on the airfoil surface areas. As future work, we believe that the parametrization models can be used for a better estimation on the surface areas due to the hidden features obtained from them.

REFERENCES

- [1] Saakaar Bhatnagar, Yaser Afshar, Shaowu Pan, Karthik Duraisamy, and Shailendra Kaushik. 2019. Prediction of aerodynamic flow fields using convolutional neural networks. *Computational Mechanics* 64, 2 (2019), 525–545.
- [2] Junfeng Chen, Jonathan Viquerat, and Elie Hachem. 2019. U-net architectures for fast prediction of incompressible laminar flows. *arXiv preprint arXiv:1910.13532* (2019).
- [3] Filipe de Avila Belbute-Peres, Thomas D. Economou, and J. Zico Kolter. 2020. Combining Differentiable PDE Solvers and Graph Neural Networks for Fluid Flow Prediction. *arXiv:2007.04439* [cs.LG]
- [4] Cihat Duru, Hande Alemdar, and Özgür Uğraş Baran. 2020. CNNFOIL: convolutional encoder decoder modeling for pressure fields around airfoils. *Neural Computing and Applications* (2020), 1–15.
- [5] Xiaoxiao Guo, Wei Li, and Francesco Iorio. 2016. Convolutional neural networks for steady flow approximation. In *Proceedings of the 22nd ACM SIGKDD International Conference on Knowledge Discovery and Data Mining*. ACM, 481–490.
- [6] Xiaowei Jin, Peng Cheng, Wen-Li Chen, and Hui Li. 2018. Prediction model of velocity field around circular cylinder over various Reynolds numbers by fusion convolutional neural networks based on pressure on the cylinder. *Physics of Fluids* 30, 4 (2018), 047105.
- [7] Sangseung Lee and Donghyun You. 2019. Data-driven prediction of unsteady flow over a circular cylinder using deep learning. *Journal of Fluid Mechanics* 879 (2019), 217–254. <https://doi.org/10.1017/jfm.2019.700>
- [8] Michael Mathieu, Camille Couprie, and Yann LeCun. 2015. Deep multi-scale video prediction beyond mean square error. *arXiv preprint arXiv:1511.05440* (2015).
- [9] Tobias Pfaff, Meire Fortunato, Alvaro Sanchez-Gonzalez, and Peter W. Battaglia. 2021. Learning Mesh-Based Simulation with Graph Networks. (2021). *arXiv:2010.03409* [cs.LG]
- [10] Vinothkumar Sekar, Chang Jiang, Qinghua and Shu, and Boo Cheong Khoo. 2019. Fast flow field prediction over airfoils using deep learning approach. *Physics of Fluids* 31, 5 (2019), 057103. <https://doi.org/10.1063/1.5094943> *arXiv:https://doi.org/10.1063/1.5094943*
- [11] Yao Zhang, Woongje Sung, and Dimitri Mavris. 2018. Application of Convolutional Neural Network to Predict Airfoil Lift Coefficient. <https://doi.org/10.2514/6.2018-1903>